

Origins of the Stereodivergent Outcome in the Staudinger Reaction between Acyl Chlorides and Imines

Ana Arrieta,[†] Begoña Lecea,[‡] and Fernando P. Cossio*[‡]

Kimika Fakultatea, Euskal Herriko Unibertsitatea, P.K. 1072, 20080 San Sebastián-Donostia, Spain, and Farmazi Fakultatea, Euskal Herriko Unibertsitatea, P.K. 450, 01080 Vitoria-Gasteiz, Spain

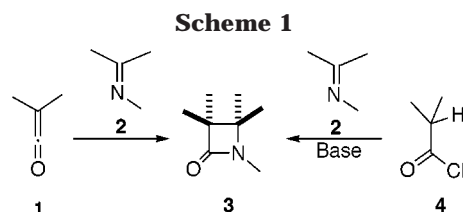
Received March 12, 1998

Calculations using density functional theory (DFT, B3LYP/6-31G* level) provide an explanation for the stereodivergent outcome observed in the Staudinger reaction between acyl chlorides and imines to form 2-azetidiones (β -lactams). When the ketene is formed prior to the cycloaddition stages, preferential or exclusive formation of cis stereoisomers is predicted. When the imine reacts directly with the acyl chloride, the step that determines the stereochemical outcome of the reaction is an intramolecular S_N2 displacement. Under these conditions, preferential or exclusive formation of trans stereoisomers is predicted, in good agreement with the experimental evidence available. It is found that both competitive processes are subjected to torquoelectronic effects. In addition, the reported calculations suggest that in both cases the polarity of the solvent enhances the diastereomeric excess of the reaction.

Introduction

Although the Staudinger reaction between ketenes and imines has been known since 1907,¹ the nature of its mechanism was not well understood until recently.² This problem was complicated with the development of different variants of the reaction, a line of research that was pioneered by Sheehan and Corey³ during their work on the chemical synthesis of penicillin derivatives. Although perhaps the most widely used methodology is the acid chloride–imine approach, several authors⁴ have reported different methodologies that allow the convergent synthesis of β -lactams (2-azetidiones) from imines and activated carboxylic acids (Scheme 1). These efforts have in turn permitted the synthesis of a wide variety of not only β -lactam antibiotics⁵ but also other biologically important compounds.⁶ More recently, the acid chloride–imine methodology has been applied to the polymer-supported synthesis of β -lactams, thus proving that this reaction is well suited for combinatorial chemistry.⁷

One of the most intriguing features of the Staudinger reaction is its different stereochemical outcome depending upon the method used in the generation of the active



species. Indeed, it has been found that the order of addition of the reactants has a profound effect on the stereochemical outcome of the reaction.⁸

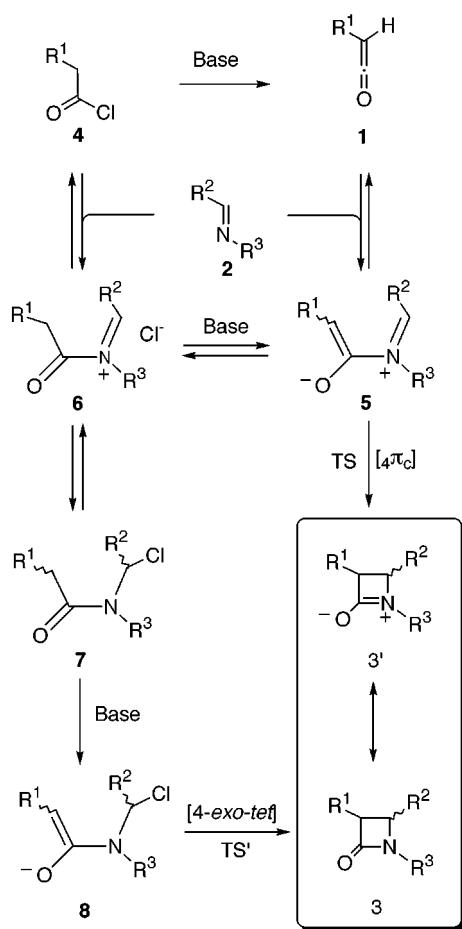
In general, it is found that when the acyl chloride is added dropwise (preferably at low temperature) over a solution of the imine and a tertiary amine, the cis cycloadduct is the major or exclusive stereoisomer detected.^{2,8} In contrast, when the tertiary base (usually triethylamine) is added over a mixture of the imine and the acyl chloride, variable mixtures of cis and trans cycloadducts are obtained, in which the *trans*-2-azetidione is the major or exclusive stereoisomer.⁸ Moreover, several experiments have shown that under the reaction conditions there is no isomerization between the cis and trans β -lactams formed,^{8a,h,9} thus proving that the distribution of diastereomers is not due to the conversion of the cis cycloadduct to the thermochemically more stable trans isomer.

Several mechanisms have been proposed in order to account for these experimental findings. After the crucial study of Lynch et al.,¹⁰ it is clear that when the acyl chloride 4 is added over the solution of the imine 2 and triethylamine formation of the corresponding ketene 1

(1) Staudinger, H. *Justus Liebigs Ann. Chem.* **1907**, 356, 51.
 (2) (a) Hegedus, L. S.; Montgomery, J.; Narukawa, Y.; Snustad, D. *J. Am. Chem. Soc.* **1991**, 113, 5748. (b) Georg, G. I.; Ravikumar, V. T. In *The Organic Chemistry of β -Lactams*; Georg, G. I., Ed.; VCH: New York, 1993; pp 331–359. (c) Tidwell, T. T. *Ketenes*; Wiley: New York, 1995; pp 518–527.
 (3) (a) Sheehan, J. C.; Ryan, J. J. *J. Am. Chem. Soc.* **1951**, 73, 1204. (b) Sheehan, J. C.; Corey, E. J. *Org. React.* **1958**, 9, 388.
 (4) For a recent survey on activating reagents in the Staudinger reaction, see: Reference 2b, pp 299–330 and references therein.
 (5) (a) Ghosez, L.; Marchand-Brynaert, J. In *Comprehensive Organic Synthesis*; Trost, B.; Fleming, I., Eds.; Pergamon: Oxford, 1991; Vol. 5, p 85. (b) Thomas, R. C. In *Recent Progress in the Chemical Synthesis of Antibiotics*; Lukacs, G., Ohno, M., Eds.; Springer: Berlin, 1988; p 533. (c) van der Steen, F. H.; van Koten, G. *Tetrahedron* **1991**, 47, 7503. (d) *Chemistry and Biology of β -Lactam Antibiotics*; Morin, R. B., Gorman, M., Eds.; Academic Press: New York, 1982; Vols. 1–3.
 (6) (a) Manhas, M. S.; Amin, S. G.; Bose, A. K. *Heterocycles* **1976**, 5, 699. (b) Manhas, M. S.; Wagle, D. R.; Chiang, J.; Bose, A. K. *Heterocycles* **1988**, 27, 1755. (c) Ojima, I. *Acc. Chem. Res.* **1995**, 28, 383.
 (7) (a) Molteni, V.; Annunziata, R.; Cinquini, M.; Cozzi, F.; Benaglia, M. *Tetrahedron Lett.* **1998**, 39, 1257. (b) Ruhland, B.; Bhandari, A.; Gordon, E. M.; Gallop, M. A. *J. Am. Chem. Soc.* **1996**, 118, 253.

(8) (a) Bose, A. K.; Anjaneyulu, B.; Bhattacharaya, S. K.; Manhas, M. S. *Tetrahedron* **1967**, 23, 4769. (b) Wells, J. N.; Lee, R. E. *J. Org. Chem.* **1969**, 34, 1477. (c) Nelson, D. A. *J. Org. Chem.* **1972**, 37, 1447. (d) Arrieta, A.; Lecea, B.; Palomo, C. *J. Chem. Soc., Perkin Trans. 1* **1987**, 845. (e) Bose, A. K.; Chang, Y. H.; Manhas, M. S. *Tetrahedron Lett.* **1972**, 4091. (f) Oshiro, Y.; Komatsu, M.; Vesaka, M.; Agawa, T. *Heterocycles* **1984**, 22, 549. (g) Doyle, T. W.; Belleau, B.; Luh, B.-Y.; Ferrari, C. F.; Cunningham, M. P. *Can. J. Chem.* **1977**, 55, 468. (h) Nelson, D. A. *J. Org. Chem.* **1972**, 37, 1447.
 (9) Barbaro, G.; Bataglia, A.; Bruno, C.; Giorgianni, P.; Guerrini, A. *J. Org. Chem.* **1996**, 61, 8480.
 (10) Lynch, J. E.; Riseman, S. M.; Laswell, W. L.; Tschaeen, D. M.; Volante, R. P.; Smith, G. B.; Shinkay, I. *J. Org. Chem.* **1989**, 54, 3792.

Scheme 2



takes place prior to the cycloaddition stages. Under these conditions, the imine **2** reacts with ketene **1** to form the zwitterionic intermediate **5** (Scheme 2).¹¹ Electrocyclic conrotatory ring closure of this intermediate leads to the corresponding β-lactam 3' ↔ **3**. This mechanism accounts for the preferential formation of *cis*-2-azetidiones when the above-mentioned protocol is used.^{2a} We¹² and Sordo et al.¹³ have found that this stereochemical outcome can be understood on the basis of the torquoelectronic effects¹⁴ that are present in the transition structure associated with the conrotatory electrocycloaddition (**TS** in Scheme 2).

Other studies, however, suggest that in the absence of base the imine **2** can react directly with the acyl chloride **4** to form the adduct **6** (Scheme 2). Low-temperature studies performed by Bose et al.¹⁵ have shown that this process is reversible. Nucleophilic addition of chloride can lead to amide **7**, which has been

isolated in several cases.^{8h,15,16} Abstraction of a proton by the tertiary amine leads to the enolate **8**, which can lead to cycloadduct **3** via an intramolecular S_N2 reaction. This latter step corresponds to a favored [4-*exo-tet*] process according to the Baldwin rules.¹⁷ However, the reasons why this latter mechanism should lead to the preferential formation of *trans* cycloadducts are not clear.

Within the above context and as an extension of our previous studies on the Staudinger reaction,¹² in the present paper we report a computational study in which the features of the transition structures associated with *both* mechanisms (**TS** and **TS'**, see Scheme 2) are reported for the first time. Our goal has been to understand the reasons underlying the different stereochemical outcome associated with both mechanisms.

Computational Methods

All the results presented in this work have been obtained using the GAUSSIAN 94¹⁸ series of programs, with the standard 6-31G* basis set.¹⁹ To include electron correlation at a reasonable computational cost, density functional theory (DFT)²⁰ has been used. We have used the hybrid three-parameter functional developed by Becke,²¹ which is usually denoted as B3LYP. This functional has been proven to yield accurate results in other thermal cycloaddition reactions.²² Zero-point vibrational energies (ZPVEs) have been computed at the B3LYP/6-31G* level and have not been scaled. All transition structures have been fully optimized and characterized by harmonic analysis.²⁵ For each located transition state, only one imaginary frequency was found in the diagonalized Hessian matrices, and the corresponding vibration was found to be associated with nuclear motion along the reaction coordinate under study.

Bond orders²⁴ and atomic charges²⁵ were calculated with the natural bond orbital (NBO) method.²⁶ Donor–acceptor interactions have also been computed by means of the NBO model, according to

(16) (a) Duran, F.; Ghosez, L. *Tetrahedron Lett.* **1970**, 245. (b) Moore, H. W.; Hernández, L.; Chambers, R. *J. Am. Chem. Soc.* **1978**, *100*, 2245.

(17) Baldwin, J. E. *J. Chem. Soc., Chem. Commun.* **1976**, 735.

(18) GAUSSIAN 94, Revision B.2: Frisch, M. J.; Trucks, G. W.; Schlegel, H. B.; Gill, P. M. W.; Johnson, B. G.; Robbb, M. A.; Cheeseman, J. R.; Keith, T.; Peterson, G. A.; Montgomery, J. A.; Raghavachari, K.; Al-Laham, M. A.; Zakrzewski, V. G.; Ortiz, J. V.; Foresman, J. B.; Peng, C. Y.; Ayala, P. Y.; Chen, W.; Wong, M. W.; Andres, J. L.; Replogle, E. S.; Gomperts, R.; Martin, R. L.; Fox, D. J.; Binkley, J. S.; Defrees, D. J.; Baker, J.; Stewart, J. P.; Head-Gordon, M.; Gonzalez, C.; Pople, J. A. Gaussian, Inc.: Pittsburgh, PA, 1995.

(19) Hehre, W. J.; Radom, L.; Schleyer, P. v. R.; Pople, J. A. *Ab Initio Molecular Orbital Theory*; Wiley: New York, 1986; pp 65–68 and references therein.

(20) (a) Parr, R. G.; Yang, W. *Density-Functional Theory of Atoms and Molecules*; Oxford: New York, 1989. (b) Bartolotti, L. J.; Fluchick, K. In *Reviews in Computational Chemistry*; Lipkowitz, K. B., Boyd, D. B., Eds.; VCH Publishers: New York, 1996; Vol. 7, pp 187–216.

(21) (a) Becke, A. D. *J. Chem. Phys.* **1993**, *98*, 5648. (b) Becke, A. D. *Phys. Rev. A* **1998**, *38*, 3098. (c) Lee, C.; Yang, W.; Parr, R. G. *Phys. Rev. B* **1980**, *37*, 785. (d) Vosko, S. H.; Wilk, L.; Nusair, M. *Can. J. Phys.* **1980**, *58*, 1200.

(22) See, for example: (a) Morao, I.; Lecea, B.; Cossio, F. P. *J. Org. Chem.* **1997**, *62*, 7033. (b) Goldstein, E.; Beno, B.; Houk, K. N. *J. Am. Chem. Soc.* **1996**, *118*, 6036. (c) Wiest, O.; Houk, K. N.; Black, K. A.; Thomas, B., IV. *J. Am. Chem. Soc.* **1995**, *117*, 8594. (d) Wiest, O.; Black, K. A.; Houk, K. N. *J. Am. Chem. Soc.* **1994**, *116*, 10336.

(23) McIver, J. W.; Komornicki, A. *J. Am. Chem. Soc.* **1972**, *94*, 2625.

(24) Wiberg, K. B. *Tetrahedron* **1968**, *24*, 1083.

(25) Wiberg, K. B.; Rabien, P. R. *J. Comput. Chem.* **1993**, *14*, 1504.

(26) (a) Foster, J. P.; Weinhold, F. *J. Am. Chem. Soc.* **1980**, *102*, 7211. (b) Reed, A. E.; Weinhold, F. *J. Chem. Phys.* **1985**, *83*, 1736. (c) Reed, A. E.; Weinstock, R. B.; Weinhold, F. *J. Chem. Phys.* **1985**, *83*, 735. (d) Reed, A. E.; Curtiss, L. A.; Weinhold, F. *Chem. Rev.* **1988**, *88*, 899.

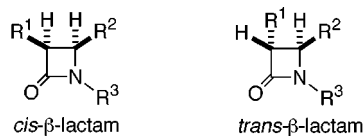
(11) Pacansky, J.; Chang, J. S.; Brown, D. W.; Schwarz, W. *J. Org. Chem.* **1982**, *47*, 2233.

(12) (a) Cossio, F. P.; Ugalde, J. M.; Lopez, X.; Lecea, B.; Palomo, C. *J. Am. Chem. Soc.* **1993**, *115*, 995. (b) Cossio, F. P.; Arrieta, A.; Lecea, B.; Ugalde, J. M. *J. Am. Chem. Soc.* **1994**, *116*, 2085. (c) Arrieta, A.; Ugalde, J. M.; Cossio, F. P.; Lecea, B. *Tetrahedron Lett.* **1994**, *35*, 4465. (d) Arrastia, I.; Arrieta, A.; Ugalde, J. M.; Cossio, F. P.; Lecea, B. *Tetrahedron Lett.* **1994**, *35*, 7825. (e) Lecea, B.; Arrastia, I.; Arrieta, A.; Roa, G.; Lopez, X.; Arriortua, M. I.; Ugalde, J. M.; Cossio, F. P. *J. Org. Chem.* **1996**, *61*, 3070.

(13) López, R.; Sordo, T. L.; Sordo, J. A.; González, J. *J. Org. Chem.* **1993**, *58*, 7036.

(14) (a) Niwayama, S.; Kallel, E. A.; Spellmeyer, D. C.; Sheu, C.; Houk, K. N. *J. Org. Chem.* **1996**, *61*, 2813. (b) Dolbier, W. R., Jr.; Korionak, H.; Houk, K. N.; Sheu, C. *Acc. Chem. Res.* **1996**, *29*, 471 and previous references therein.

(15) Bose, A. K.; Spiegelman, G.; Manhas, M. S. *Tetrahedron Lett.* **1971**, 3167.

Scheme 3^a

- 3a** R¹=R²=R³=H
3b R¹=Cl; R²=CH₃; R³=H
3c R¹=R²=CH₃; R³=H
3d R¹=Cl; R²=CH=CH₂; R³=CH₃

^a Only one enantiomer is drawn.

$$\Delta E_{\phi\phi^*}^{(2)} = -n_{\phi} \frac{\langle \phi^* | \hat{F} | \phi \rangle^2}{\epsilon_{\phi^*} - \epsilon_{\phi}} \quad (1)$$

where n_{ϕ} is the occupation number of the donor NBO, \hat{F} is the Fock operator, and ϕ and ϕ^* are two filled and unfilled NBOs having ϵ_{ϕ} and ϵ_{ϕ^*} energies, respectively. Although the NBO analysis has been extensively used within the Hartree–Fock (HF) theory, its extension to DFT is controversial, since the φ_i Kohn–Sham (KS) orbitals and their energies ϵ_i have in general no strict physical significance.²⁷ However, according to Kohn, Becke and Parr,²⁷ “... all ϵ_i and φ_i are of great semiquantitative value, much like Hartree–Fock energies and wave functions, often more so, because they reflect also correlation effects, and are consistent with the exact physical density.” Within this context, we have computed frontier MO’s and the $\Delta E_{\phi\phi^*}^{(2)}$ values at both HF and B3LYP levels.²⁸ However, we would like to emphasize that these data have only semiquantitative value.

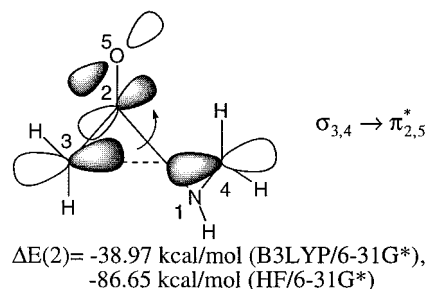
Nonspecific solute–solvent interactions were simulated using the self-consistent isodensity polarization model (SCIPCM) as implemented by Wiberg.²⁹ The solvent considered in these calculations has been dichloromethane ($\epsilon = 9.08$, ϵ being the relative permittivity constant³⁰), since most of the experimental studies have been carried out in this solvent.

The plots of molecular orbitals have been performed using the MOLDEN program.³¹

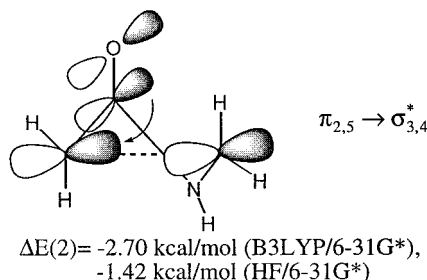
Results and Discussion

The transition structures included in this study are those associated with the formation of the cycloadducts *cis*- and *trans*-**3a–d** reported in Scheme 3. These structures correspond to computationally accessible equivalents of the substituents usually present in previous experimental work. The chief geometric features of the parent transition structure **TSa** are reported in Figure 1. These structural data are similar to those found at other theoretical levels^{12,13} and clearly show the conrotatory nature of the torsion around the N1–C4 and C2–C3 bonds. The shape of the frontier molecular orbitals (FMO’s) of the **TSa** was found to be virtually identical at both the HF/6-31G* and B3LYP/6-31G* levels, although the corresponding orbital energies were different in magnitude (Figure 2). Inspection of the FMOs of **TSa**

(see Figure 2) reveals that they arise from the combination of the HOMO of the ketene^{12a} and the π_{CN}^* LUMO of an imine. The HOMO of **TSa** is dominated by a bonding interaction between C3 and C4. This bond in formation can act as a good electron donor given the high value of the energy of the HOMO. Similarly, the LUMO is a very good electron acceptor and is dominated by an antibonding interaction between C3 and C4. The NBO analysis assigns a σ localized bond between C3 and C4, and the donating ability of $\sigma_{3,4}$ takes place mainly through a two-electron interaction with the π^* orbital between C2 and O5:



Similarly, the electron acceptor ability of $\sigma_{3,4}^*$ takes place mainly via donation from the $\pi_{2,5}$ bond, although this interaction is less efficient than the former:



Therefore, although the FMOs of **TSa** are different from those computed for the saddle point associated with the cyclobutene ring cleavage,¹⁴ the conrotatory geometry of the former and the nature of the interaction between C3 and C4 give rise to torquoelectronic effects. The *E* geometry of the starting imine³² determines the inward disposition of the substituent at C4 (emphasized by a black arrow in Figure 1), whereas the inward or outward orientation of the substituent at C3 is determined by the mode of approach between the ketene and the imine and will determine the *cis/trans* stereochemistry of the reaction.^{12,13} The transition structures resulting from several substituted ketenes and imines are reported in Figure 3, in which the *E* geometry of the imine³² has been preserved. The corresponding relative energies are reported in Table 1.

In the case of *cis* and *trans*-3-chloro-4-methyl-2-azetidinone, the B3LYP/6-31G*+ Δ ZPVE level of theory predicts that the *cis*-**TSb** transition state in which the chlorine is in an outward orientation is 8.29 kcal/mol more stable than the *trans*-**TSb** in which the chlorine is directed inward. The HF/6-31G*+ Δ ZPVE level of theory agrees with this prediction but yields a slightly lower energy difference, 7.40 kcal/mol. This results in the

(27) Kohn, W.; Becke, A. D.; Parr, R. G. *J. Phys. Chem.* **1996**, *100*, 12974.

(28) For several recent papers reported combined B3LYP and NBO studies, see, for example: (a) Glendening, E. D.; Hrabal, J. A. *J. Am. Chem. Soc.* **1997**, *119*, 12940. (b) Krapp, J.; Remko, M.; Schleyer, P. v. R. *Inorg. Chem.* **1997**, *36*, 4241. (c) García, A.; Cruz, E. M.; Sarasola, C.; Ugalde, J. M. *J. Phys. Chem. A* **1997**, *101*, 3021.

(29) (a) Wiberg, K. B.; Castejon, H.; Keith, T. A. *J. Comput. Chem.* **1996**, *17*, 185. (b) Wiberg, K. B.; Keith, T. A.; Frisch, M. J.; Murcko, M. *J. Phys. Chem.* **1995**, *99*, 9073. (c) Wiberg, K. B.; Rablen, P. R.; Rush, D. J.; Keith, T. A. *J. Am. Chem. Soc.* **1995**, *117*, 4261.

(30) Reichardt, C. *Solvents and Solvent Effects in Organic Chemistry*; VCH Publishers: Weinheim, 1990.

(31) Schaftenaar, G. *MOLDEN-A Package for Displaying Molecular Density*; CAOS/CAMM Center Nijmegen: Toernooiveld, Nijmegen, The Netherlands, 1991.

(32) (a) Guerra, A.; Lunazzi, L. *J. Org. Chem.* **1995**, *60*, 7959. (b) Warren, C. H.; Wettermark, G.; Weis, K. *J. Am. Chem. Soc.* **1971**, *93*, 4658. (c) Patai, S., Ed. *The Chemistry of the Carbon–Nitrogen Double Bond*; Wiley: New York, 1970.

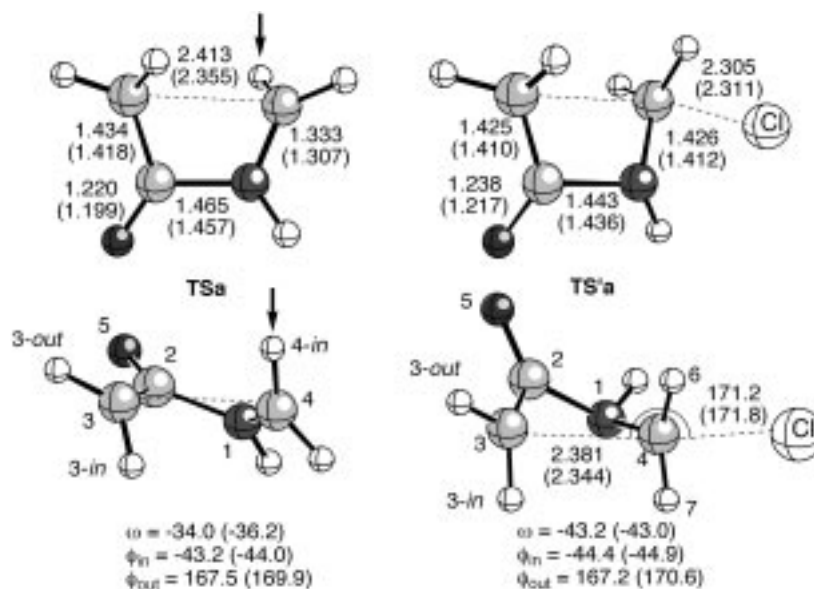


Figure 1. Fully optimized (B3LYP/6-31G* level) transition structures **TSa** and **TS'a**. The ω , ϕ_{in} and ϕ_{out} dihedral angles are defined as follows: $\omega = \text{C3-C2-N1-C4}$, $\phi_{in} = \text{R}_{in}\text{-C3-C2-N1}$, and $\phi_{out} = \text{R}_{out}\text{-C3-C2-N1}$. Bond distances and angles are given in Å and deg, respectively. Unless otherwise stated, atoms are represented by increasing order of shadowing as follows: H, C, O, N. Numbers in parentheses correspond to HF/6-31G* values.

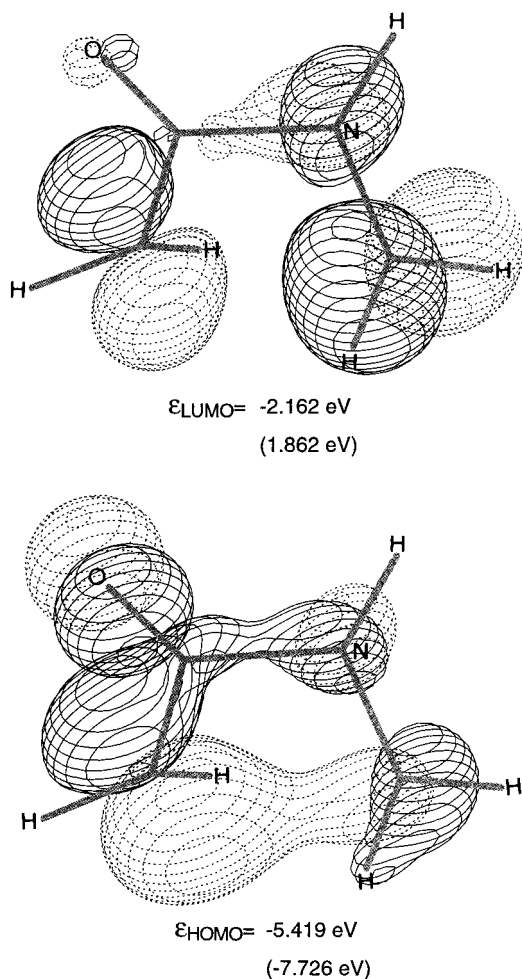
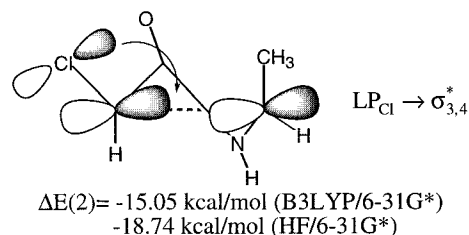


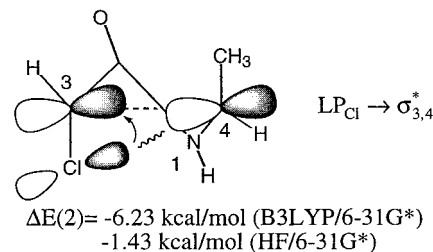
Figure 2. Frontier MO's of **TSa** computed at the B3LYP/6-31G* level. The contour plot is 0.065 au. Numbers in parentheses correspond to HF/6-31G* values.

preferential formation of the *cis* cycloadducts, in good agreement with the experimental observations.^{2,8} The

NBO analysis shows that in *cis-TSb* there is a very efficient two-electron interaction between a lone pair of the *outward* chlorine and the $\sigma_{3,4}^*$ NBO:



In contrast, in *trans-TSb* there is a four-electron interaction between one lone pair of the *inward* chlorine and the $\sigma_{3,4}$ localized orbital. In addition, the $\text{LP}_{\text{Cl}} \rightarrow \sigma_{3,4}^*$ donation is now less efficient because of the unfavored overlap between one lone pair of the chlorine atom and the *p* AO at C4:



To minimize these destabilizing interactions, the C3–C4 bond distance is enlarged with respect to the *cis* analogue (see Figure 3). These combined factors result in the relative stabilization of *cis-TSb*. However, it is noteworthy that the $\Delta E_{in-out} = E(in) - E(out)$ energy difference is lower in our case than in the electrocyclic ring cleavage of 3-chlorocyclobutene. Houk et al.^{14a} have reported a value of $\Delta E_{in-out} \approx 14 \text{ kcal/mol}$ for the latter reaction. We attribute this relatively low destabilization of the *inward* chlorine in the Staudinger reaction to two factors: First, the π_{CO} bond in *trans-TSb* is almost

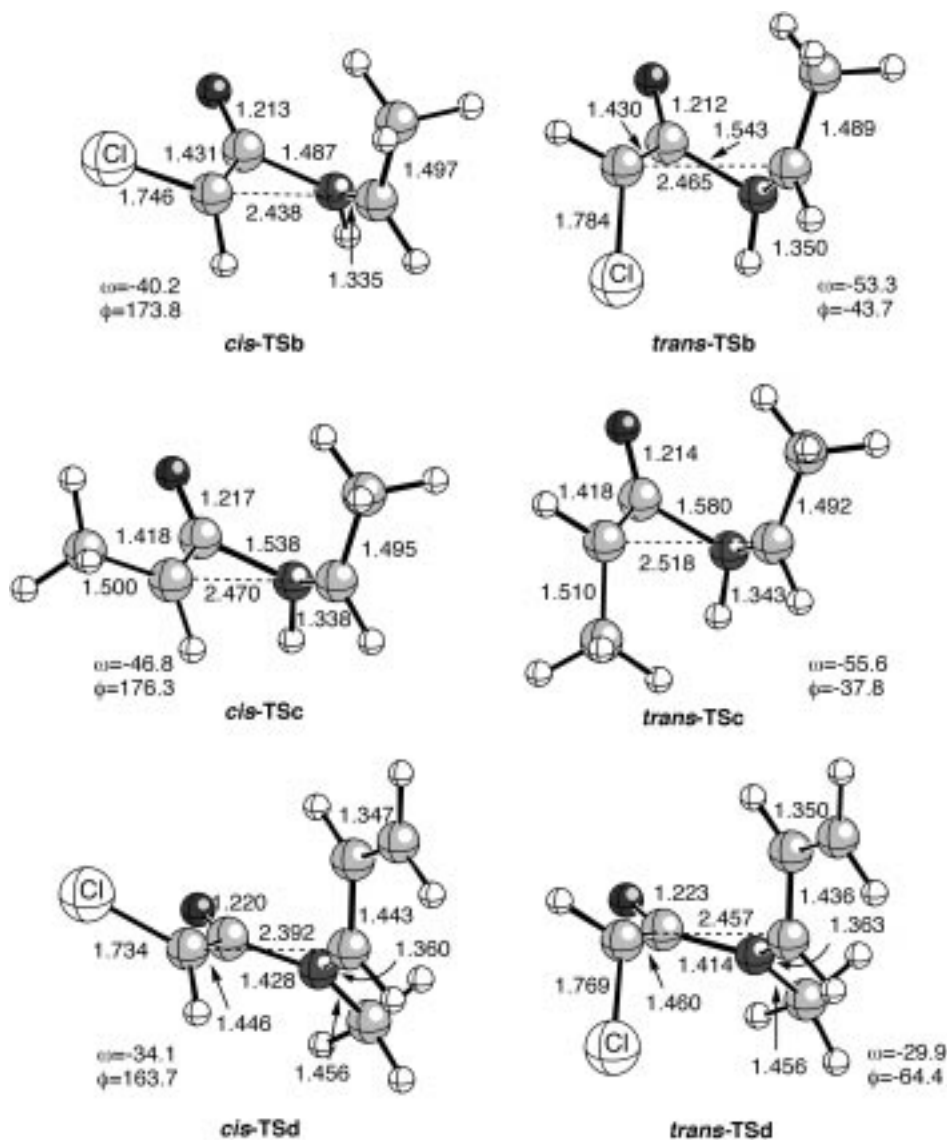
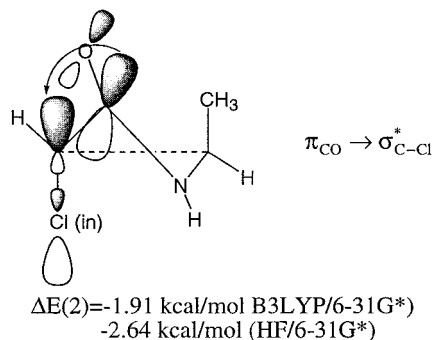


Figure 3. Fully optimized (B3LYP/6-31G* level) transition structures **TSb-d**. See Figure 1 caption for additional details.

parallel to the σ_{C-Cl} bond, thus permitting a relatively efficient $\pi_{CO} \rightarrow \sigma_{C-Cl}^*$ donation, not accessible to *cis-TSb*:



This also results in a higher C3–Cl bond distance for *trans-TSb* (see Figure 3). Second, in *cis-TSb* there is a repulsive Coulombic interaction between the O5 atom, with a Mulliken charge of -0.478 , and the *outward* chlorine. This almost parallel arrangement between the C2–O5 and C3–Cl dipoles results in a higher dipole moment for *cis-TSb*. The dipole moments computed at the B3LYP/6-31G* level are 6.27 and 3.77 D for *cis*- and

trans-TSb, respectively. This difference in polarity should promote a higher ΔE_{in-out} difference in solution. In effect, our SCIPCM results show that *trans-TSb* is 11.57 kcal/mol less stable than *cis-TSb* in dichloromethane solution, a value 3.34 kcal/mol higher than that found in vacuo (see Table 1). Although there are no systematic studies on the stereochemical outcome of the Staudinger reaction in different solvents, our calculations suggest that torquoselectivity should increase with the polarity of the solvent.

The ΔE_{in-out} values for *cis*- and *trans-TSc* that incorporate a methyl group at C3 are found to be 7.22 and 7.56 kcal/mol in vacuo and in solution, respectively. The NBO analysis yields results similar to those found for **TSb** but lower in magnitude, given the lower donor ability of the σ_{CC} bond with respect to a chlorine lone pair (The σ_R^o Taft values for chlorine and methyl are -0.23 and -0.11 , respectively).³³ Similarly, the low polarity of the C3–Me bond results in very similar ΔE_{in-out} values in the gas phase and in solution.

We have also computed the *cis*- and *trans-TSd* saddle points, in which there is a methyl group at N1 and an *inward* vinyl group at C4, to mimic the behavior of

Table 1. Total Energies^a (–au) and Relative Energies^{a,b} (in Parentheses, kcal/mol) of Transition Structures **TSb–d** and **TS'b–d**

entry	structure	R ¹	R ²	R ³	TS- <i>cis</i>	TS- <i>trans</i>	TS'- <i>cis</i>	TS'- <i>trans</i>
$\epsilon = 1.00$								
1	b	Cl	CH ₃	H	746.019 71 (0.00)	746.006 59 (+8.23)	1206.304 78 (0.00)	1206.314 86 (–6.32)
2	c	CH ₃	CH ₃	H	325.701 65 (0.00)	325.690 15 (+7.22)	785.979 15 (0.00)	785.988 16 (–5.65)
3	d	Cl	CH=CH ₂	CH ₃	823.390 47 (0.00)	823.375 39 (+9.46)	1283.663 61 (0.00)	1283.676 91 (–8.34)
$\epsilon = 9.08$								
4	b	Cl	CH ₃	H	746.034 25 (0.00)	746.015 81 (+11.57)	1206.364 74 (0.00)	1206.379 20 (–9.07)
5	c	CH ₃	CH ₃	H	325.712 64 (0.00)	325.700 59 (+7.56)	786.045 51 (0.00)	786.056 99 (–7.20)
6	d	Cl	CH=CH ₂	CH ₃	823.400 69 (0.00)	823.383 69 (+10.67)	1283.725 81 (0.00)	1283.741 48 (–9.83)

^a Energies computed at the B3LYP/6-31G*/B3LYP/6-31G*+ Δ ZPVE level. When $\epsilon = 9.08$, the energies have been evaluated at the B3LYP(SCIPCM)/6-31G*/B3LYP/6-31G*+ Δ ZPVE level. ^b Computed with respect to the *cis* transition structures.

benzylidene or cinnamylidene imines. In *cis*-**TSd**, the *outward* chlorine at C3 induces a relative stabilization with respect to *trans*-**TSd** of 9.46 kcal/mol in vacuo and 10.67 kcal/mol in dichloromethane solution. These results are quite similar to those found for *cis*- and *trans*-**TSb**, and both the NBO analysis and the relative dipole moments are in agreement with the above discussion for *cis*- and *trans*-**TSb**.

In summary, our calculations indicate that, if the Staudinger reaction takes place via the ketene–imine route, torquoelectronic effects induce preferential or exclusive formation of the *cis* cycloadducts in good agreement with the experimental data available. These effects can be enhanced by increasing the polarity of the solvent and/or that of the substituent at C3.

We have also located and characterized the parent saddle point **TS'a** associated with the intramolecular S_N2 reaction. The chief geometric features of this transition structure are also reported in Figure 1 and reveal a fair agreement between the HF/6-31G* and B3LYP/6-31G* structural parameters. Inspection of these data reveals an almost linear arrangement between the C3, C4, and Cl atoms, with a departure of ca. 9° from linearity. The calculated H6–C4–N1–H7 dihedral angle is 160.0° at the B3LYP/6-31G* level, thus suggesting that **TS'a** is not a “halfway” transition structure. The NBO analysis assigns a charge of –0.325 to the C3 atom. The NBO charges of the C4 and Cl atoms are +0.309 and –0.584, respectively, thus indicating that this saddle point is highly ionic in nature. Streitwieser³⁴ and Bader³⁵ have found similar results in acyclic S_N2 transition structures.

The FMOs of **TS'a** are reported in Figure 4. These MOs arise from the contribution of the HOMO of an enolate and the LUMO of an alkyl halide, the latter being mainly a σ_{CX}^* orbital. Thus, the HOMO of **TS'a** is dominated by the enolate moiety, whereas the LUMO has a large contribution of a *p* AO of C4, as we must expect from the cationic character of this atom. Therefore, the FMOs of the parent saddle point associated with the 4-*exo-tet* process are very different from those found for its electrocyclic congener **TSa**. However, the 2-azetidione parts of both transition structures are topologically

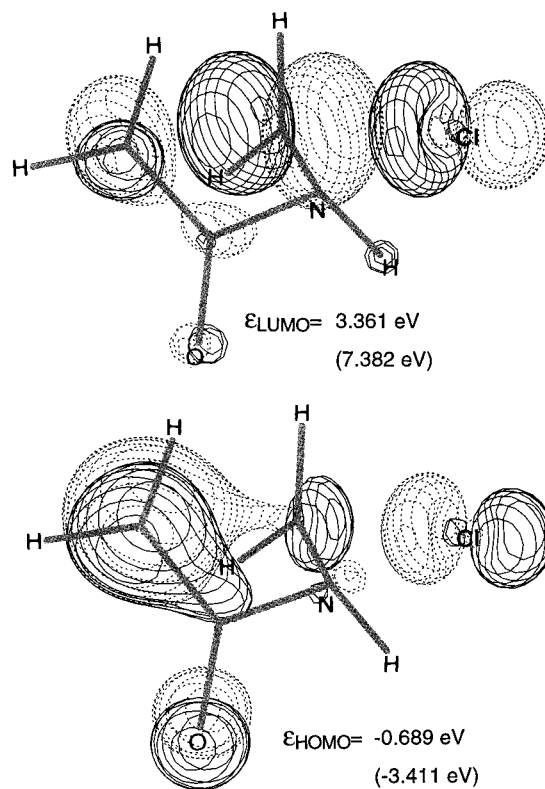


Figure 4. Frontier MO's of **TS'a** computed at the B3LYP/6-31G* level. The contour plot is 0.065 au. Numbers in parentheses correspond to HF/6-31G* values.

related to each other. The main difference is that in the S_N2 process there is no conrotatory restriction to the torsion around the N1–C4 bond. However, both the [4 π c] and the [4-*exo-tet*] reactions require rotation around the C2–C3 bond to proceed.

In principle, substitution at the four positions available in **TS'a** should lead to four stereoisomeric transition structures. However, only two diastereomeric pairs were found when the candidate structures were submitted to optimization, since the remaining possible structures could not be located or converged to those that we report here. These transition structures are shown in Figure 5. As can be seen, substitution at C4 promotes a departure from linearity in the arrangement between the C3–C4 and C4–Cl bonds, larger than that observed in the parent **TS'a**. In addition, this substitution stabilizes

(33) (a) Taft, R. W.; Lewis, I. C. *J. Am. Chem. Soc.* **1958**, *80*, 2436. (b) Ehrenson, S.; Brownlee, R. T. C.; Taft, R. W. *Prog. Phys. Org. Chem.* **1973**, *10*, 1.

(34) Streitwieser, A.; Choy, G. S.-C.; Abu-Hasanayn, F. *J. Am. Chem. Soc.* **1997**, *119*, 5013.

(35) Bader, R. F. W. *Can. J. Chem.* **1986**, *64*, 1036.

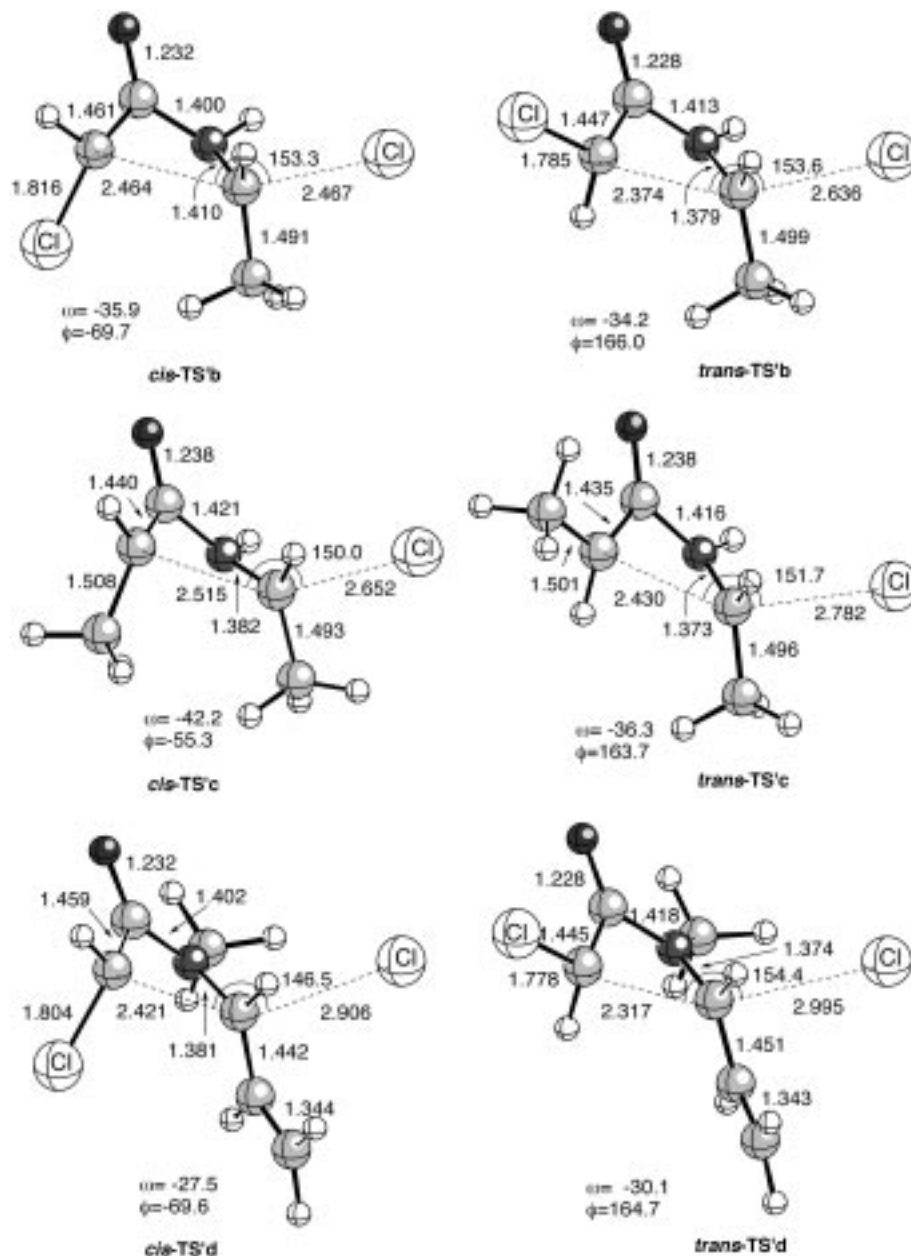


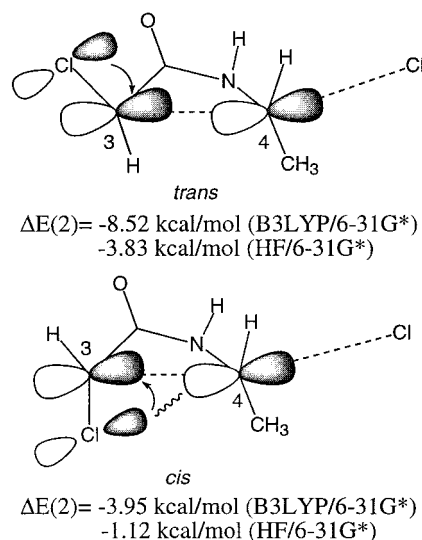
Figure 5. Fully optimized (B3LYP/6-31G* level) transition structures **TS'b–d**. See Figure 1 caption for additional details.

the electron-deficient character of C3, thus yielding larger C4–Cl and/or C3–C4 bond distances (see Figures 1 and 5).

In the case of **TS'b**, our calculations indicate that the *trans* transition structure is 6.32 and 9.07 kcal/mol more stable than its *cis* analogue in vacuo and in dichloromethane solution, respectively (see Table 1). Inspection of the second-order perturbational analysis of the NBOs reveals that in *trans-TS'b* the donation of one lone pair of chlorine to the $\sigma_{3,4}^*$ orbital is more efficient than in *cis-TS'b*:

Again, it is found that in *cis-TS'b* the Cl–C3 bond distance is larger than in *trans-TS'b* because of the more efficient $\pi_{2,5} \rightarrow \sigma_{CCl}^*$ donation in the former saddle point. This effect is also found in **TS'c** and **TS'd**. Therefore, torquoelectronic effects also play a significant role in this reaction.

Another consequence of the geometries of *cis*- and *trans-TS'b* is that in the latter the relative orientation of the C3–Cl and C2–O5 bonds results in a larger dipole



moment. Thus, the computed dipole moments of *cis*- and *trans*-**TS'b** are 4.437 and 6.182 D, respectively. As a consequence, the energy gap between both transition structures is enhanced when solvent effects are included (see Table 1).

The remaining diastereomeric transition structures **TS'c** and **TS'd** show similar features. In *cis*- and *trans*-**TS'c**, the lower donating ability of the methyl group results in a lower relative stabilization of the *trans* isomer. In the case of **TS'd**, the orientation of the vinyl group at C4 promotes an allylic stabilization of this center. It is noteworthy that in this case the relative stabilization of the *cis* saddle point is larger than those calculated in the preceding cases, both in the gas phase and in solution.

Therefore, the S_N2 intramolecular mechanism clearly favors the preferential or exclusive formation of *trans*-2-azetidinones. This stereochemical outcome is favored when the reaction between an acyl chloride and an imine are allowed to interact in the absence of a tertiary base in the initial stages of the reaction.

Conclusions

In this paper, we report a comparative study of two competitive reaction paths that can operate in the reaction between acyl chlorides and imines. From the reported results, the following conclusions can be drawn:

(i) The electrocyclic conrotatory ring closure of the second step of the Staudinger reaction favors the preferential or exclusive formation of the *cis* cycloadduct. This stereoselection is determined by the *E* geometry of the imine and its limited torsion in the conrotatory transition structure, as well as by the two-electron interaction between a filled orbital of the substituent at C3 and the $\sigma_{3,4}^*$ orbital. In addition, the *cis* transition structures are more polar than their *trans* congeners. Therefore, solvent effects enhance the energy difference in favor of

formation of *cis* cycloadducts. This stereochemical outcome agrees with that observed in the reaction between imines and acyl halides that are transformed in ketenes prior to the cycloaddition stages.

(ii) The S_N2 route involves free rotation around the N1–C4 bond and torsion around the C2–C3 bond. The resulting transition structures are quite ionic in character and are also subjected to torquoelectronic effects. In this case, the same factors involved in the pericyclic route favor the preferential formation of the *trans* isomers. Solvent effects also enhance the energy gap between both diastereomeric transition structures. This stereochemical outcome is that observed when the acyl chloride is allowed to react with the imine prior to the addition of the tertiary base.³⁶

Acknowledgment. This work has been supported by the Secretaría de Estado de Universidades, Investigación y Desarrollo (project PB96-1481), and by the Gobierno Vasco/Eusko Jaurlaritza (project GV 170.215-EX97/11). We thank Dr. Joseph Fowler for helpful discussions during the elaboration of this manuscript

Supporting Information Available: Cartesian coordinates of all the structures reported in this work (6 pages). This material is contained in libraries on microfiche, immediately follows this article in the microfilm version of the journal, and can be ordered from the ACS; see any current masthead page for ordering information.

JO9804745

(36) Quite recently, Bose et al. have reported that in the microwave-assisted reaction between acyl chlorides and imines the amount of *trans* cycloadducts is usually larger than that obtained under classical thermal conditions. A possible explanation for this result is that under microwave irradiation the route involving direct reaction between the acyl chloride and the imine competes more efficiently with the ketene–imine reaction path. See: Bose, A. K.; Banik, B. K.; Manhas, M. S. *Tetrahedron Lett.* **1995**, *36*, 213. See also: Bose, A. K.; Sayaraman, M.; Okawa, A.; Bari, S. S.; Robb, E. W.; Manhas, M. S. *Tetrahedron Lett.* **1996**, *37*, 6989.